

Nanotoxicology

ISSN: 1743-5390 (Print) 1743-5404 (Online) Journal homepage: https://www.tandfonline.com/loi/inan20

Superparamagnetic iron oxide nanoparticles (SPIONs) modulate hERG ion channel activity

Roberta Gualdani, Andrea Guerrini, Elvira Fantechi, Francesco Tadini-Buoninsegni, Maria Rosa Moncelli & Claudio Sangregorio

To cite this article: Roberta Gualdani, Andrea Guerrini, Elvira Fantechi, Francesco Tadini-Buoninsegni, Maria Rosa Moncelli & Claudio Sangregorio (2019) Superparamagnetic iron oxide nanoparticles (SPIONs) modulate hERG ion channel activity, Nanotoxicology, 13:9, 1197-1209, DOI: 10.1080/17435390.2019.1650969

To link to this article: https://doi.org/10.1080/17435390.2019.1650969

Published online: 22 Aug 2019.

Submit your article to this journal

Article views: 32

View related articles

View Crossmark data

Full Terms & Conditions of access and use can be found at
https://www.tandfonline.com/action/journalInformation?journalCode=inan20

NANOTOXICOLOGY
2019, VOL. 13, NO. 9, 1197–1209
https://doi.org/10.1080/17435390.2019.1650969

Taylor & Francis
Taylor & Francis Group

ARTICLE

Check for updates

Superparamagnetic iron oxide nanoparticles (SPIONs) modulate hERG ion channel activity

Roberta Gualdani[a,b], Andrea Guerrini[a], Elvira Fantechi[a], Francesco Tadini-Buoninsegni[a], Maria Rosa Moncelli[a] and Claudio Sangregorio[a,c]

[a]Dipartimento di Chimica "Ugo Schiff", Università di Firenze, Sesto Fiorentino, Italy; [b]Institute of Neuroscience, Laboratory of Cell Physiology, Université Catholique de Louvain, Brussels, Belgium; [c]ICCOM-CNR and INSTM, Sesto Fiorentino, Italy

ABSTRACT

Superparamagnetic iron oxide nanoparticles (SPIONs) are widely used in various biomedical applications, such as diagnostic agents in magnetic resonance imaging (MRI), for drug delivery vehicles and in hyperthermia treatment of tumors. Although the potential benefits of SPIONs are considerable, there is a distinct need to identify any potential cellular damage associated with their use. Since human ether à go-go-related gene (hERG) channel, a protein involved in the repolarization phase of cardiac action potential, is considered one of the main targets in the drug discovery process, we decided to evaluate the effects of SPIONs on hERG channel activity and to determine whether the oxidation state, the dimensions and the coating of nanoparticles (NPs) can influence the interaction with hERG channel. Using patch clamp recordings, we found that SPIONs inhibit hERG current and this effect depends on the coating of NPs. In particular, SPIONs with covalent coating aminopropylphosphonic acid (APPA) have a milder effect on hERG activity. We observed that the time-course of hERG channel modulation by SPIONs is biphasic, with a transient increase (~20% of the amplitude) occurring within the first 1–3 min of perfusion of NPs, followed by a slower inhibition. Moreover, in the presence of SPIONs, deactivation kinetics accelerated and the activation and inactivation I–V curves were right-shifted, similarly to the effect described for the binding of other divalent metal ions (e.g. Cd^{2+} and Zn^{2+}). Finally, our data show that a bigger size and the complete oxidation of SPIONs can significantly decrease hERG channel inhibition. Taken together, these results support the view that Fe^{2+} ions released from magnetite NPs may represent a cardiac risk factor, since they alter hERG gating and these alterations could compromise the cardiac action potential.

ARTICLE HISTORY
Received 25 January 2019
Revised 27 June 2019
Accepted 26 July 2019

KEYWORDS
SPIONs; hERG channel; cardiotoxicity; iron nanoparticles

1. Introduction

Superparamagnetic iron oxide nanoparticles (SPIONs) have been largely investigated in the recent past as they represent one of the most promising candidates for the application of nanotechnology in biomedicine. SPIONs are composed of nanosized synthetic γ-Fe_2O_3 (maghemite) or Fe_3O_4 (magnetite) particles, with mean size below 50 nm, and, since are biocompatible, are one of the few examples of clinically approved metal oxide nanoparticles (NPs). The strong interest on these systems relies on the possibility of exploiting their unique properties, in a wide range of biomedical applications, including magnetic resonance imaging (MRI), targeted delivery of drugs or genes, tissue engineering, hyperthermia therapy, magnetic transfections and chelation therapy (Colombo et al. 2012; Theranostic Nanomedicine: Special Issue 2011; Huber 2005; Gupta and Gupta 2005; Johannsen et al. 2007; Maier-Hauff et al. 2011; Bulte et al. 2001). Indeed, SPIONs have the unique property of superparamagnetism, and are able to generate heat in alternating magnetic fields, to enhance contrast in MRI and to target specific tissues or organs by control of an external magnetic field gradient. Moreover, the nanometer size and large surface/volume ratio of SPIONs provide many advantages, such as enhanced reactivity, permeability across biological membranes and tissue barriers. On the other hand, the same nanoscale properties can potentially induce cytotoxicity by impairing the functions of the major components of the cell, e.g. DNA, mitochondria and nucleus (Dissanayake, Current, and Obare

CONTACT Roberta Gualdani roberta.gualdani@uclouvain.be Institute of Neuroscience, Laboratory of Cell Physiology, Université Catholique de Louvain, av. Mounier 53, box B1.53.17, B-1200 Brussels, Belgium; Claudio Sangregorio csangregorio@iccom.cnr.it ICCOM-CNR and INSTM, via Madonna del Piano 10, 50019 Sesto Fiorentino (FI), Italy

© 2019 Informa UK Limited, trading as Taylor & Francis Group

2015; Moore et al. 2015). In fact, exposure to SPIONs has been associated with significant toxic effects such as inflammation, apoptosis, impaired mitochondrial function and genotoxicity (Veranth et al. 2007; Hafeli et al. 2009; Jeng and Swanson 2006; Hussain et al. 2005; Stroh et al. 2004). To reduce the toxicity and improve the biocompatibility, SPIONs are, often, coated with polymers, such as dextran, lipids, polyethylene glycol, and polyvinyl alcohol. Different coatings provide distinct chemical properties, metabolism, toxicity, and biodistribution (Duguet et al. 2006).

One of the mechanisms by which SPIONs can induce health effects is *via* the generation of ROS. Following internalization through a number of possible mechanisms, SPIONs are presumably degraded into iron ions within the lysosomes by hydrolyzing enzymes at low pH (Singh et al. 2010). 'Free' Fe^{2+} ions can potentially cross the nuclear or mitochondrial membrane and, in the latter case, can react with hydrogen peroxide and oxygen produced by the mitochondria to produce highly reactive hydroxyl radicals and ferric ions (Fe^{3+}) via the Fenton reaction:

$$Fe^{2+} + H_2O_2 \rightarrow Fe^{3+} + \dot{O}H + OH$$

Therefore, hydroxyl radicals generated by the free Fe^{2+} could damage DNA, proteins, polysaccharides and lipids *in vivo* (Singh et al. 2010).

Considering the recent dramatic growth of biomedical applications of SPIONs, there is an urgent need to fully address all relevant biocompatibility and biosafety issues associated with their usage and exposure.

In the last years, many international agencies working on global health, e.g. European Medicines Agency (EMEA), World Health Organization (WHO), and Food and Drug Administration (FDA), have realized the importance to evaluate adverse health effects of NPs, once they enter the body.

One of the major hurdles in the development of new drugs is the reduction of risk of drug-induced cardiac arrhythmia. For this reason, the investigation of human ether à go-go-related gene (hERG) channel blockage represents a fundamental step in the drug discovery process.

hERG encodes the pore-forming subunit of the K^+ channel and is responsible for the rapid component of the delayed-rectifier K^+ current (I_{Kr}) in the heart (Sanguinetti et al. 1996). As a consequence, impairment in expression or function of hERG channel leads to cardiac long-QT syndrome, which could be due to gene mutation (Mitcheson et al. 2000), off-target drug block (Fermini and Fossa 2003), or post-translational modifications of channel proteins (Chen, Helliwell, and Clare 2009). This has led to the removal of several drugs from the market and represents a significant issue in the development of new drugs (Fermini and Fossa 2003). Therefore, new drug candidates must be tested for a potential inhibitory effect on the hERG current as a first step in a nonclinical testing strategy (Food and Drug Administration, HHS, 2005), since hERG blockage is considered an indicator of potential pro-arrhythmic risk.

The interaction of nanomaterials and ion channels has been scarcely investigated to date. This is rather surprising since the patch-clamp technique is a fast and well-established screening method for preclinical drug validation. It has been demonstrated that phosphine-stabilized gold NPs with 1.5 nm core size blocked irreversibly hERG channels, whereas thiol-stabilized Au-NPs of similar size had no effect *in vitro* and *in vivo* (Leifert et al. 2013). Recently, Piscopo and Brown (2018) studied the different effects of ZnO and $ZnCl_2$ NPs on hERG channel gating, concluding that ZnO NPs alter hERG rectification. Moreover, Gu et al. (2018) showed that MoS_2 nanoflakes are able to stably bind three K^+ channels, KcsA, Kir3.2, and $K_V1.2$, through distinct binding modes that involve the selectivity filter and the voltage sensing domain of the channels.

Conversely, to date, despite the fundamental role SPIONs are expected to play in the biomedical field, there is no indication about their effect on ion channels, and more specifically, on hERG channel. In order to fill this gap and improve the understanding of the potential toxicity of SPIONs we present here an investigation aimed at evaluating the effects of SPIONs on hERG channel activity. To this purpose, the effect of SPIONs with different size, surface coating, and oxidation state on hERG K^+ current was investigated. The obtained results allowed us to evaluate a possible mechanism of hERG channel inhibition by SPIONs involving the release of Fe^{2+} ions, which depends on NP size and coating. More in general they demonstrate the efficacy of the gold standard patch-clamp technique

as a screening method to assess the potential cardiotoxicity of nanomaterials.

2. Materials and methods

2.1. Maintenance of mammalian cell lines and cell transfection

Patch-clamp studies were carried out on Human Embryonic Kidney (HEK) 293 cells stably transfected with hERG channel (DI.V.A.L. Toscana SRL, Sesto Fiorentino (FI), Italy). Cells were plated in 12 mm round coverslips 24 h before patch-clamp recordings.

2.2. Electrophysiological recordings

Electrophysiological recordings were performed in whole-cell patch-clamp configuration. The extracellular solution had the following composition: 140 mM NaCl, 5 mM KCl, 1 mM $MgCl_2$, 2 mM $CaCl_2$, 10 mM Glucose, 10 mM HEPES, pH 7.4 with NaOH. The pipette contained: 130 mM KCl, 10 mM EGTA, 1 mM $MgCl_2$, 2 mM Mg-ATP, 10 mM HEPES, pH 7.20 with KOH. Solutions were applied to the cell *via* a gravity-fed perfusion system coupled with a Fast Exchange Open Diamond Bath chamber (VC-6 Six Channel Valve Controller, Warner Instruments, Hamden, CT), in order to allow very fast solution exchange. Currents were sampled at 20 kHz and digitally filtered at 2.9 kHz. The currents were not corrected for the liquid junction potential. Series resistance was electronically compensated. Patch-clamp recordings of cell cultures were carried out at room temperature 48 h after transfection. Patch-clamp electrodes were pulled from Sutter capillary glass (Novato, San Francisco, CA, USA) on a Flaming/Brown type puller (Sutter P-87), and fire polished to 3–4 MΩ resistance, using a microforge (Narishige, Tokyo, Japan). For recordings a Multiclamp 700B amplifier (Molecular Devices Inc., Sunnyvale, CA, USA) and Digidata 1440 data acquisition board (Molecular Devices Inc., Sunnydale, CA, USA) with pCLAMP 10 software (Molecular Devices Inc., Sunnyvale, CA, USA) were used. Data analysis was performed using Origin version 8.0 (OriginLab Corporation, Northampton, MA, USA).

2.3. SPIONs synthesis and characterization

SPIONs were synthesized by thermal decomposition of metal-organic precursors in high boiling solvent, in the presence of surfactants: Iron(III) acetylacetonate (2 mmol), oleylamine (8 mmol), and oleic acid (8 mmol) were dissolved in Benzilether (50 mL) and stirred under nitrogen flow for 15 min at room temperature; the mixture was heated at 200 °C for 30 min and then to 300 °C for 30 or 60 min to produce NPs of 8 nm (in the following labeled as NP8) or 13 nm (NP13), respectively. The mixture was cooled down to room temperature and the oleic acid coated, black SPIONs, were magnetically separated, washed with ethanol and suspended in toluene. For each batch of SPIONs the oleic acid coating was removed and NPs were either left uncoated or covered by the hydrophilic ligand Poly(Acrylic Acid) (PAA), 2-3 DiMercaptoSuccinic Acid (DMSA), or 3-Aminopropylphosphonic Acid (APPA). Uncoated SPIONs (NP*x*-OH, where $x = 8$ or 13 according to the average size) were prepared by mixing the toluene SPION suspension with a tetramethylammonium hydroxide (TMAOH) water solution 25% and sonicating for 15 min. The SPIONs were magnetically separated, washed with ethanol and suspended in water at 10 mg/mL concentration; to improve the stability the pH was corrected to 8 by a small addition of NaOH 0.1 M. Water soluble SPIONs were prepared by mixing the toluene SPION suspension (5 mg/mL) with equivalent amount of PAA in tetrahydrofuran (NP*x*-PAA), DMSA in dimethyl sulfoxide (NP*x*-DMSO), or APPA and TMAOH (2:1 w/w) in water (NP*x*-APPA), and sonication for 1 h. SPIONs were magnetically separated, washed with ethanol and suspended in water. All the processes were carried out in inert atmosphere to prevent magnetite oxidation. Ligand exchange was verified by FTIR spectroscopy performed using a Perkin Elmer Spectrum BX. One half of freshly prepared suspensions of NP8 and NP13 were converted to the fully oxidized spinel ferrite (maghemite) by gently bubbling air in the suspenions (NP8ox and NP13ox samples). The NPs underwent the same ligand exchange procedures described for oleic acid coated Fe_3O_4 NPs. The size distribution of NP8 and NP13 was investigated by transmission electron microscopy using a CM12 PHILIPS microscope operating at 100 kV. Samples were prepared

by drop drying a diluted suspension of SPIONs in hexane onto 200 mesh carbon-coated copper grids. Powder XRD patterns were recorded with a Bruker D8 Advance diffractometer equipped with a CuKα radiation and operating in θ–θ Bragg Brentano geometry at 40 kV and 40 mA. Zeta potential was measured on diluted water suspensions using a Zetasizer Nano (Malvern Instruments Ltd, Malvern, UK) apparatus. X-band (9.41 GHz) Electron Paramagnetic Resonance (EPR) spectra were recorded on the surnatant of NP8-DMSA after ligand exchange reaction and separation of the NPs, with a Bruker E500 spectrometer equipped with an ESR900 (Oxford Instruments, Abingdon, UK) continuous-flow 4He cryostat and a SHQ resonator. The absence of the ferromagnetic resonance absorption peak in the room temperature EPR spectra confirmed the complete removal of SPIONs. ICP-AES measurements were performed in triplicate by a Varian 720-ES Inductively Coupled Plasma Atomic Emission Spectrometer (ICP-AES).

The quantitative analysis of iron ion released by the SPIONs was carried out with an inductively coupled plasma mass spectrometer (ICP-MS, Agilent 7700, Agilent Technologies, Santa Clara, CA) on the water suspensions obtained after removal of the iron oxide NPs by dialysis. The calibration standards were prepared from a commercial standard mix solution (Enviromental spike mix 5183-4687 Agilent) with a nominal iron concentration of 1000 mg/mL.

3. Results

3.1. SPIONs modulate hERG channel activity

Monodisperse SPIONs of different size were successfully prepared by thermal decomposition of iron acetylacetonate. The average size, estimated from the analysis of TEM micrographs, was found equal

Table 1. Mean diameter from statistical analysis of TEM micrograph (d_{TEM}); Average crystal size (d_{XRD}) and lattice parameter before (a) and after oxidation (a_{ox}), obtained from the XDR pattern fit with Pawley method using T.O.P.A.S.® software. Lattice parameter for bulk Fe_3O_4 and γ-Fe_2O_3 are 8.3960 Å (PDF 19-0629) and 8.3515 Å (PDF 39-1346), respectively.

Sample	dTEM (nm)	dXRD (nm)	a (Å)	aox (Å)
NP8	8.0 ± 0.9	9.3	8.407 (3)	8.363 (2)
NP13	13.5 ± 1.9	12.1	8.396 (3)	8.378 (9)

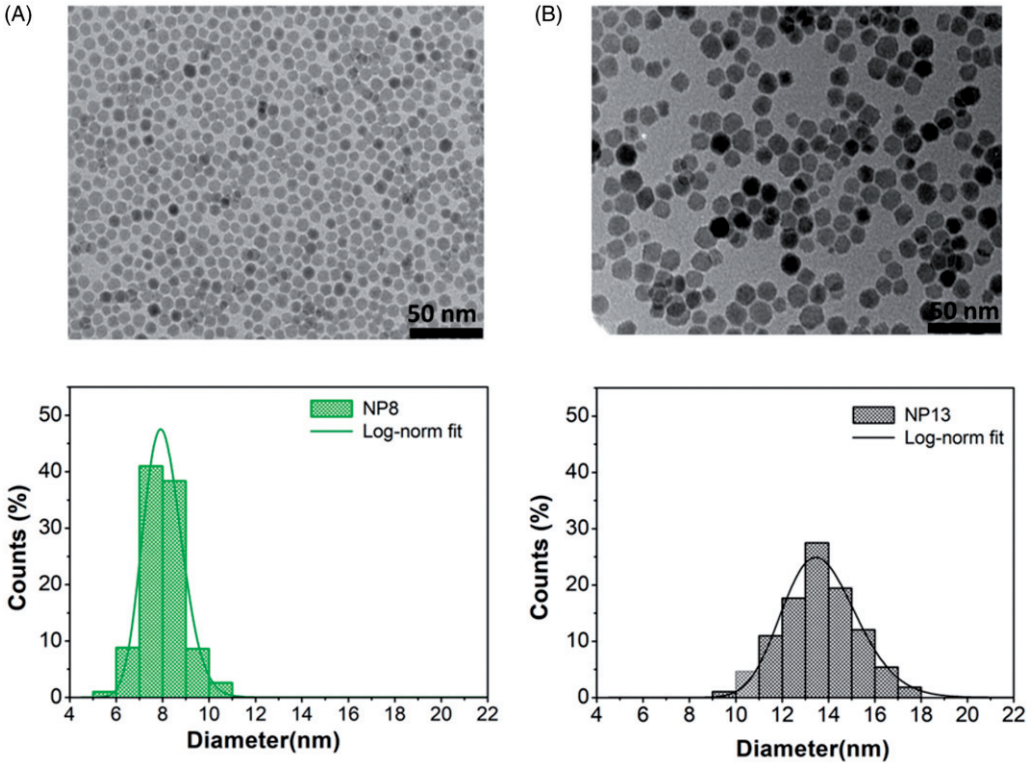

Figure 1. Selected TEM micrographs of NP8 (left) and NP13 (right) and the corresponding size distribution obtained by a statistical analysis over more than 100 NPs; the thick lines are the fit to a log normal function with d_{LN}=8.0 ± 0.8 nm (NP8) and d_{LN}=13.6 ± 1.7 nm (NP13).

to 8.0 ± 0.9 and 13.5 ± 1.9 nm for NP8 and NP13, respectively (Figure 1). The Rietveld analysis of the X-ray diffraction patterns (Table 1) demonstrated the NPs are single-phase monocrystals with the cubic spinel ferrite structure of magnetite (Fe_3O_4 $a = 8.3970(1)$ Å). For both samples the oleic acid coating was replaced with APPA, PAA, or DMSA ligands by simple ligand exchange process under inert atmosphere to prevent core oxidation. For each series, a fourth sample was prepared by removing the organic coating by treatment with TMAOH. The effectiveness of the procedure was demonstrated by the change of solubility of the NPs (from hydrophobic to hydrophilic) and by FTIR spectroscopy (data not shown). The stability of the water suspensions was controlled by Zeta-potential measurement. For all the investigated samples large negative values, in the −25/−50 mV range, were observed (Table 2) indicating the occurrence of a negative surface charge, which is responsible for the observed suspensions' stability.

Table 2. Zeta-potential values of water suspensions of NP8 and NP13 coated with APPA, DMSA, PAA, or OH.

Zeta-potential (mV)				
	APPA	DMSA	PAA	OH
NP8-*x*	−26 ± 1	−33 ± 2	−41 ± 1	−46 ± 2
NP13-*x*	−28 ± 2	−31 ± 1	−48 ± 2	−43 ± 2

To investigate the effect of SPIONs on hERG potassium channel, we performed patch-clamp experiments on HEK cells heterologously expressing the hERG channel. The concentration selected for the experiments (40 μM in Fe ions) was chosen in the range where iron oxide NPs can be considered biocompatible, i.e. below 100 μg/mL (Singh et al. 2010; Ankamwar et al. 2010). To elicit the activating outward current, a depolarizing step from a holding potential of −80 to 0 mV (3 s in duration) was applied. Tail current was evoked by repolarizing to −40 mV for 3 s. Successive command pulses were applied at 10-s intervals. Our data show that NP8 SPIONs, coated with different ligands, modulate differently hERG channel activity. In particular, SPIONs non coated (NP8-OH) or coated by the organic ligands poly(acrylic acid) (NP8-PAA) and 2,3-dimercaptosuccinic acid (NP8-DMSA) strongly inhibit hERG channel (Figure 2(A–C)), whereas SPIONs coated by the 3-aminopropyl phosphonic acid (NP8-APPA) have a mild inhibitory effect (Figure

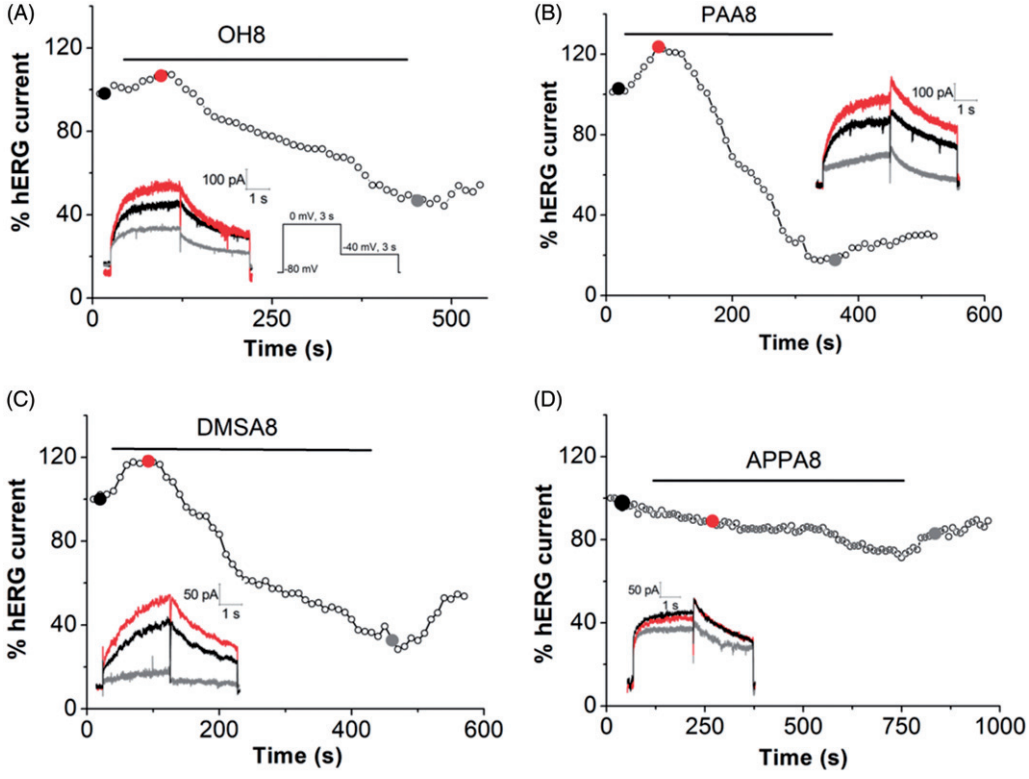

Figure 2. Time course of hERG tail current inhibition in the presence of SPIONs-Fe_3O_4: 40 μM NP8-OH (A), 40 μM NP8-PAA (B), 40 μM NP8-DMSA (C), and 40 μM NP8-APPA (D). The insets show hERG currents recorded at the indicated time intervals in the time course, before (black trace), and after 2 min (red trace) or 5 min (gray trace) of SPIONs perfusion.

2(D)). The time-course of hERG channel modulation by SPIONs is bi-phasic: a transient increase (∼20%) occurring within the first 3 min of NPs perfusion is followed by a slower inhibition. This trend is more evident for NP8-OH, NP8-DMSA, and NP8-PAA (Figure 2(A–C)). Moreover, after 10 min of SPIONs perfusion, the residual hERG current in the presence of NP8-APPA was ∼ %70, whereas NP8-OH, NP8-PAA, and NP8-DMSA caused 64 ± 6%, 78 ± 8%, and 77 ± 7% of hERG current inhibition, respectively. In the absence of the treatment the current recorded in whole cell configuration is quite stable for several minutes (data not shown).

3.2. Oxidation state and dimension of SPIONs affect hERG channel inhibition

SPIONs of maghemite (γFe_2O_3), obtained through controlled oxidation of the corresponding Fe_3O_4 SPIONs, have a milder effect on hERG channel, compared to non-oxidized SPIONs (Figure 3(A–C)). In particular, the iron oxidation has a dual effect on the time course of the hERG tail current recorded in the presence of SPIONs: the transient increase, observed in Figure 2(A–C), affecting the initial phase of time course disappeared and the inhibition phase was significantly reduced. Finally, we examined the effects of SPION size on hERG channel activity: SPIONs with a core of 13 nm (NP13) have a significantly smaller effect with respect to NP8. In agreement with our previous results on NP8, SPIONs NP13 non-covered or coated by PAA or DMSA have the strongest effect on hERG channel, compared to SPIONs NP13 covered by APPA. The results are summarized in Figure 3(D–E).

3.3. SPIONs modulate hERG channel gating

To understand the mechanism of action of SPIONs on hERG channel, we studied the effect of SPIONs on the kinetics of the hERG currents, with a special attention to activation and deactivation currents, as

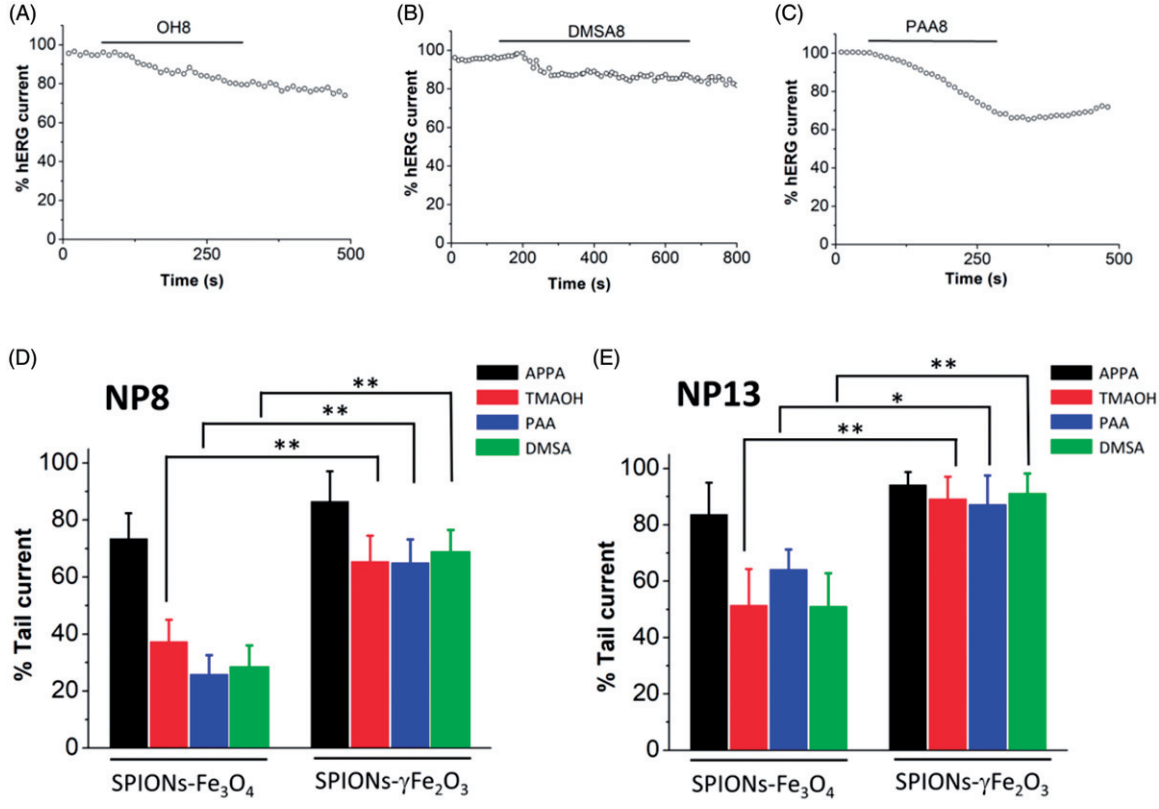

Figure 3. Time course of hERG tail current inhibition in the presence of SPIONs-γFe_2O_3 (NPox): 40 μM NP8ox-OH (A), 40 μM NP8ox-DMSA (B), 40 μM NP8ox-PAA (C). Mean relative hERG currents amplitude in the presence of 40 μM SPION NP8 (D) and 40 μM SPION NP13 (E). Each graph shows the results obtained in the presence of magnetite (SPIONs-Fe_3O_4) and maghemite (SPIONs-γFe_2O_3) SPIONs coated by different ligands. Each column represents the mean ± SEM of $n = 8$ cells. $^{**}p < 0.01$, $^{*}p < 0.05$ (two-way ANOVA test).

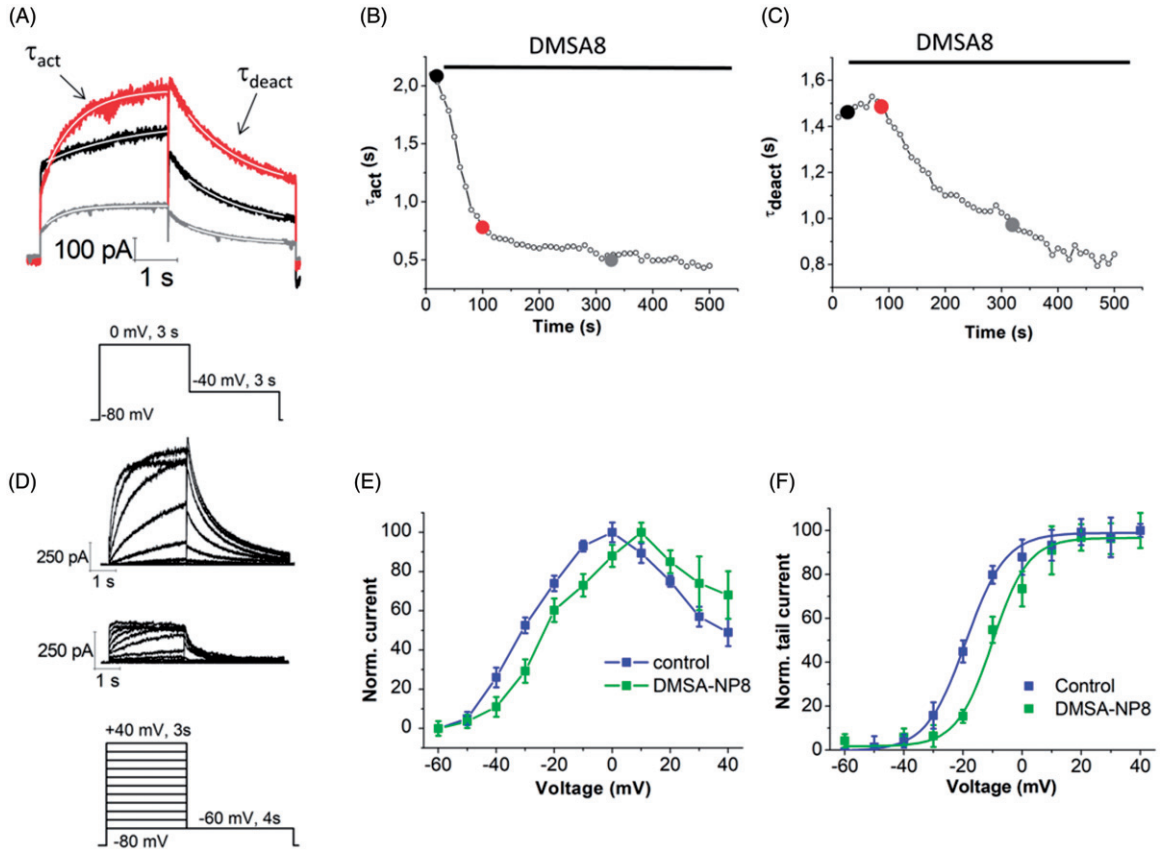

Figure 4. (A) Representative hERG currents obtained before (black trace), at 2 min of SPIONs perfusion (red trace) and after 5 min (gray trace) of SPIONs perfusion of 40 μM NP8-DMSA. Time course of SPIONs effects on hERG activation (τ_{act}, B) and deactivation (τ_{deact}, C) time constants. (D) Representative steady-state hERG currents recorded using the pulse protocol shown, in the absence (top panel) and in the presence (middle panel) of NP8-DMSA. Depolarizing steps (3 s) were applied from a holding potential of −80 mV, to test potentials from −60 to 40 mV in 10 mV increments. Normalized (with respect to the control currents) I–V relationships for current measured at the end of the test pulse (E) and at the tail current peaks (F), before (control) and after addition of NP8-DMSA. I–V relationships for tail current amplitudes were fitted with a Boltzmann function. $V_{1/2}$ shifted from −19.7 ± 1.6 mV (control) to −8.8 ± 2.0 mV ($p < 0.05$, paired *t*-test; $n = 6$ cells).

shown in Figure 4(A). We plotted the time course of τ_{act}, obtained by mono-exponential fitting of the rising phase of the activation current (Figure 4(B)), and τ_{deact}, extrapolated by fitting the hERG tail current (Figure 4(C)) (Sanguinetti et al. 1995; Zhou et al. 1998). To elicit the activation current, a depolarizing step from a holding potential of −80 to 0 mV (3 s in duration) was applied. Tail current was evoked by repolarizing to −40 mV for 3 s. We observed that the activation and deactivation kinetics had not a parallel evolution. In fact, the reduction in τ_{act} (which is usually associated with an increase of hERG current) preceded the reduction in τ_{deact} (which, on the contrary, is associated with a decrease of hERG current) by about 2–3 min. In particular, τ_{act} decreased in the first 2–3 min of recording (Figure 4(B)). At the same time, τ_{deact} slightly increased in the first 3 min of perfusion and then decreased (Figure 4(C)). The trend of both τ_{act} and τ_{deact} explain the bi-phasic time-course observed in Figure 2, where a transient increase of the current was followed by a slower inhibition.

The presence of SPIONs affects the I–V relationship of hERG activation current. The voltage-dependence of SPIONs-induced inhibition was measured on hERG K^+ current amplitudes, similarly to what previously described (Gualdani et al. 2015; Gualdani et al. 2018) (Figure 4(D)). Tail currents were elicited by repolarization to −60 mV, normalized to the maximal control amplitude and fitted with a Boltzmann function (Figure 4(F)). The presence of NP8-DMSA caused a right-shift of the I–V relationship of hERG activation current (Figure 4(E)). Moreover, the voltage required for half-maximal activation ($V_{1/2}$) was shifted in the

presence of NP8-DMSA, from -19.7 ± 1.6 to -8.8 ± 2.0 mV (Figure 4(F)).

It is worth noting that the observed behaviors do not appear to be related to the surface charge, which, according to Zeta-potential measurements, is rather similar throughout the series of investigated samples.

3.4. Effect of SPIONs on hERG inactivation

Steady-state inactivation currents were measured following the protocol reported in Figure 5(A) as described in Ficker, Jarolimek, and Brown (2001): channels were inactivated at +60 mV and, to recover the channels from inactivation, short test pulses from −100 to +20 mV were applied. Depolarization to +60 mV after these test pulses evoked a large outward inactivating current. Figure 5(A) shows sample traces of inactivating current I_{hERG} in the absence (control) and in the presence of NP8-DMSA. Current amplitudes measured after +60 mV depolarization step were normalized, plotted against membrane voltage and fitted by a Boltzmann function. Our data indicate that NP8 covered by DMSA causes a right shift of the steady-state inactivation. $V_{1/2}$ values extrapolated from the curves shifted from -55.4 ± 1.3 mV (control) to -31.2 ± 2.0 mV (Figure 5(B)).

3.5. SPIONs modulate hERG channel activity through Fe^{2+} release

To investigate whether the overall effect of SPIONs on hERG current could be associated with the release of metal ions from the magnetic core to the extracellular solution and the subsequent binding of the metal ions to hERG channel, the amount of 'free' iron ions in solution was evaluated by ICP after separation from the SPIONs by dialysis (Table 3). The concentration of Fe in solution was found much higher for NP8 non-covered (OH^-) or covered by DMSA or PAA, compared to NP8-APPA. Moreover, NPs with a core of 13 nm (NP13) globally released less Fe in solution, suggesting that the smaller surface to volume ratio increases the chemical stability of NPs. Interestingly, the iron ions released into the solution by magnetite SPIONs NP8-DMSA, which caused the highest inhibitory effect, are mostly in the lower oxidation state, Fe^{2+}. This is shown in Figure 6(A) where the EPR signal recorded on the dyalized solution freshly prepared (red trace) and after 5 days of air exposure (black trace), is reported. The freshly prepared solution did not show any transition, as expected for Fe^{2+} ions, while after 5 days a sharp transition at $g = 4.3$, attributable to high spin Fe^{3+} ions in rhombic symmetry, was clearly visible.

To confirm the specificity of the effect of Fe^{2+} on hERG channel with respect to its oxidized form Fe^{3+}, we tested the affinity of both ions on hERG current (Figure 6(C,D)). Unexpectedly, we observed that Fe^{2+} inhibits hERG current with higher affinity, compared to Fe^{3+} ions. The IC_{50} values extrapolated from the Hill curve are 143 ± 10 and 780 ± 19 μM, for Fe^{2+} and Fe^{3+}, respectively (Figure 6(B)).

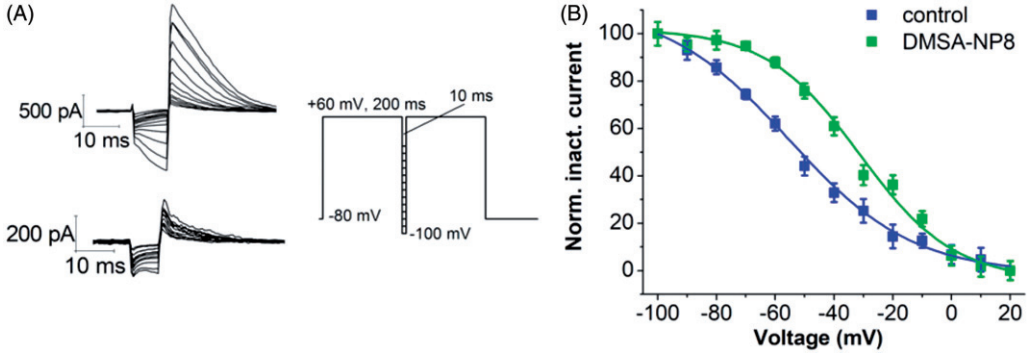

Figure 5. (A) Representative hERG traces, in the absence (top panel) and in the presence (bottom panel) of NP8-DMSA, elicited by the voltage protocol shown in the middle panel, testing steady-state inactivation currents. (B) Normalized (with respect to the control currents) steady-state I–V inactivation curves, before (control) and after addition of NP8-DMSA. Data are expressed as mean ± SEM; error bars for some points are masked by symbols. Solid lines represent fits with Boltzmann function. $V_{1/2}$ shifted from -55.4 ± 1.3 mV (control) to -31.2 ± 2.0 mV ($p < 0.01$, paired t-test; $n = 6$ cells).

4. Discussion

Exposure to SPIONs has been associated with significant toxic effects such as inflammation, apoptosis, impaired mitochondrial function, and genotoxicity. To evaluate the cardiac toxicity of SPIONs, we investigated the effect of SPIONs on hERG channel activity. Since hERG channel controls cardiac beat stability, this study has implications for the choice of NPs to be used in biomedicine.

Divalent and trivalent metal ions affect the activity of voltage-gated ion channels, with multiple effects: they can block the pore (Armstrong, Swenson, and Taylor 1982); they can bind to surface charges (McLaughlin 1989); they can bind allosterically to specific sites outside the pore and alter the gating properties of the channels (Beedle, Hamid, and Zamponi 2002; Elinder and Arhem 2003).

Concerning hERG channel, Ca^{2+} and Mg^{2+} reduce the rate of activation, increase the rate of deactivation and induce a positive shift in the voltage dependence of activation (Johnson, Mullins, and Bennett 1999; Johnson, Balser, and Bennett 2001; Po et al. 1999; Lin and Papazian 2007). Transition metal ions (e.g. Cd^{2+}, Co^{2+}, Ni^{2+}, and Zn^{2+}) have similar effects on hERG channel gating. Cd^{2+}, for example, reduces the rate of activation, increases the rate of deactivation and shifts the $V_{1/2}$ of activation and inactivation to more positive voltages (Fernandez et al. 2005).

To date, the effect of iron ions on ion channels has been poorly investigated. It has been shown that Fe^{2+} acts as pore blocker and permeant ion of L-type Ca^{2+} channel (Winegar, Kelly, and Lansman 1991; Tsushima et al. 1999). In addition, Fe^{2+} has significant effects on channel gating, like other

Table 3. Free iron ion concentration detected by ICP-MS in SPION suspensions with initial iron oxide concentration of 1 mg/mL.

Concentration of Fe (μM)				
	APPA	DMSA	PAA	OH^-
NP8-*x*	0.27	2.50	2.74	9.98
NP13-*x*	0.25	2.78	0.19	0.17
NP8ox-*x*	0.77	3.88	2.38	5.62
NP13ox-*x*	0.56	3.14	0.42	0.80

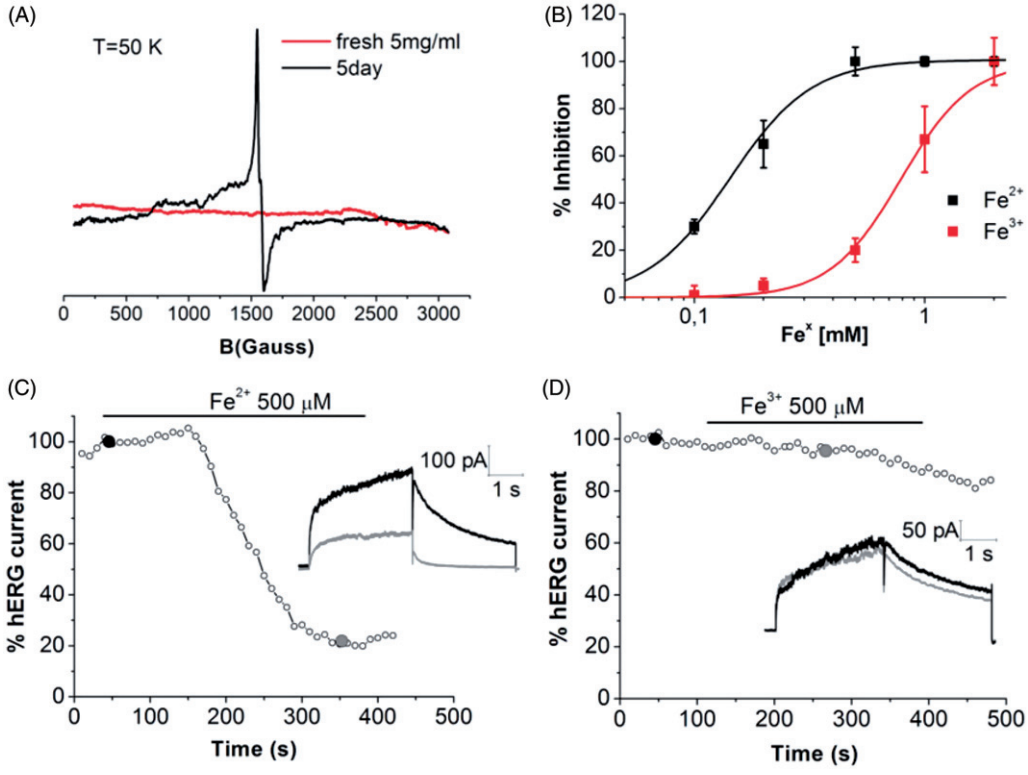

Figure 6. (A) EPR spectra of a NP8-DMSA water suspension after complete removal of the magnetic NPs. Spectra were collected at 50 K immediately after the ligand exchange reaction (red curve), and 5 days later (black curve). (B) Concentration-response relationship (mean ± SEM) for block of hERG tail current by Fe^{2+} and Fe^{3+} ($n = 6$ per data point). Time course of hERG tail current inhibition in the presence of 500 μM Fe^{2+} (C) and Fe^{3+} (D). The insets show hERG currents recorded at the indicated time intervals in the time course. A depolarizing step of 3 s was applied from a holding potential of −80 to 0 mV. Tail current was generated by repolarizing to −40 mV for 3 s.

divalent cations (Elinder and Arhem 2003). However, there are no publications describing the interaction between hERG channel and iron ions.

Our data showed that magnetite SPIONs accelerate deactivation kinetics of hERG current and cause a right-shift of the activation and inactivation I–V curves, similarly to the effect described for the binding of other metal ions on hERG channel. Moreover, we observed that bigger size (NP13), covalent coating (APPA ligand) and complete oxidation of SPIONs decrease the inhibitory effect on hERG channel.

ICP analysis of iron content in the dialyzed suspension of SPIONs revealed that the 'free' iron concentration in the extracellular medium is strongly correlated with the degree of hERG inhibition: (i) with the exception of DMSA coated sample, the amount of Fe released is lower in NP13, compared to the NP8 samples (Table 3) and (ii) for the NP8 series, SPIONs coated by APPA released a lower amount of Fe, compared to the other coatings (Table 3). On the other hand, oxidized SPIONs released a comparable amount of iron, compared to non-oxidized NPs. However, we observed a significant shift in the affinity of hERG channel for Fe^{2+} and Fe^{3+} (the IC_{50} values are, respectively, 143 ± 10 and $780 \pm 19\,\mu M$) that could explain the milder effect of maghemite SPIONs on hERG current (Figure 3(D,E)).

Puzzling our data together, we hypothesized that Fe^{2+} released from the inorganic core is the main responsible for the strong hERG inhibition by magnetite SPIONs. Recently, Piscopo and Brown (2018) showed that ZnO NPs exert an effect on hERG channel either through a direct interaction or through an interaction with the lipid environment of the hERG channel. Moreover, they excluded an effect due to the release of Zn^{2+}, since the concentration of free Zn^{2+} in solution was found to be negligible compared to the IC_{50} value extrapolated from the dose-response curve of Zn^{2+}.

Similarly, our data showed that the 'free' Fe^{2+} concentration is significantly lower (0.2–10 μM) compared to the IC_{50} value measured in Fe^{2+} solution without NPs. However, we found an unexpected strong correlation between patch-clamp data and ICP measurements that led us to hypothesize that 'free' Fe^{2+} could play an active role in hERG channel inhibition, even if this role seems to be dependent on SPION presence. Based on our results, we may speculate that SPIONs can interact with the lipid environment, change the physical properties of the membrane affecting hERG channel function, as suggested in a recent review (Kudaibergenova, Perissinotti, and Noskov 2018), and synergically enhance the effect of free Fe^{2+} on hERG channel.

Finally, we observed that the time-course of hERG channel current modulated by SPIONs is bi-phasic, showing a transient increase (∼20%) occurring within the first 3 min of perfusion of NPs followed by a slower inhibition. This biphasic effect (Figure 2) could be explained by the fact that the activation and deactivation kinetics had not a parallel evolution, suggesting that the two phases of hERG inhibition are not associated with the same intracellular phenomena. More specifically, the reduction in τ_{act} preceded the reduction in τ_{deact} (Figure 4(B,C)), as observed previously (Bérubé, Caouette, and Daleau 2001), after external application of H_2O_2 on cells expressing hERG channel. We hypothesized that the first phase of hERG inhibition could be due to the modulation of hERG channel by ROS, produced via Fenton reaction by 'free' Fe^{2+}, as previously described in Taglialatela et al. (1997). They showed that exposure of *Xenopus* oocytes to an extracellular solution containing $FeSO_4$ and ascorbic acid, which accelerates lipid peroxidation and ROS production, caused a significant increase of hERG outward K^+ currents and a depolarizing shift of the voltage dependence of channel inactivation.

To corroborate our hypothesis, we observed that the transient increase disappeared when we perfused maghemite SPIONs (Figure 3(A–C)), suggesting that it could be specifically due to the presence of 'free' Fe^{2+}.

Iron homeostasis is tightly regulated in the body (Zhang and Enns 2009). Increased intracellular iron concentration has been associated with cardiac (Horwitz and Rosenthal 1999; Kremastinos and Farmakis 2011) and neuronal disorders (Stankiewicz and Brass 2009), including amyotrophic lateral sclerosis, Parkinson's disease, and Alzheimer's disease (Andrews 1999; Oshiro, Morioka, and Kikuchi 2011). In myocardial cells, iron overload affects cellular structure (Iancu et al. 1987), gene expression (Parkes et al. 2000), and Na^+ and K^+ channel properties (Kuryshev

et al. 1999). Moreover, the presence of iron into the body leads to the production, via the Fenton reaction, of highly reactive hydroxyl radicals that cause oxidative damage to DNA, lipids, and proteins. Our study suggests that Fe^{2+} ions released from magnetite NPs may represent a cardiac risk factor, since they alter hERG gating and these alterations could compromise the cardiac action potential.

In conclusion, we investigated the effect of water suspensions of SPIONs characterized by different size, coating, or oxidation state (magnetite or maghemite) of the inorganic core, on the activity of hERG channel. This protein plays a crucial role in the repolarization of cardiac action potential and regulation of the heartbeat and it is therefore an ideal system for preclinical cardiotoxicity testing of new drugs and nanomaterials. Using patch-clamp recordings, we found that Fe_3O_4 NP suspensions have an inhibitory effect on the hERG current, which depends on the size (the larger the size, the smaller the effect) and on the coating of the magnetic NPs. Conversely, almost no inhibition of the hERG channel was observed when the NPs were converted to the fully oxidized spinel, maghemite.

Overall, our results support the conclusion that SPIONs have no direct inhibitory effect on hERG channel, the observed blocking effect being more likely related to 'free' ferrous ions released by the iron oxide NPs, whose extent depends upon the kind of coating and the size of the NPs. Therefore, SPIONs are not potentially cardiotoxic, provided they are fully oxidized, and the proper coating is selected. Importantly, we used the well-established patch-clamp technique as a predictable and efficient screening method for emerging materials like SPION-based nanocomposite to be used in biomedical applications.

Acknowledgments

The authors acknowledge Michele Petrecca for the help to record FTIR spectra and Martin Albino for ICP-MS measurements. Patch-clamp measurements were performed at the RISE A-MeProLab of the Department of Chemistry 'Ugo Schiff' (University of Florence).

Disclosure statement

The authors declare no conflict of interest.

Funding

Financial support from Fondazione Cassa di Risparmio di Firenze and FAS (Fondo Aree Sottoutilizzate) 2007–2013 project are gratefully acknowledged.

ORCID

Roberta Gualdani http://orcid.org/0000-0003-3617-4953
Andrea Guerrini http://orcid.org/0000-0002-7621-1029
Elvira Fantechi http://orcid.org/0000-0002-9323-2198
Francesco Tadini-Buoninsegni http://orcid.org/0000-0001-5594-2554
Claudio Sangregorio http://orcid.org/0000-0002-2655-3901

References

Andrews, N. C. 1999. "Disorders of Iron Metabolism." *The New England Journal of Medicine* 341(26): 1986–1995. doi:10.1056/NEJM199912233412607.

Ankamwar, B., T. C. Lai, J. H. Huang, R. S. Liu, M. Hsiao, C. H. Chen, and Y. K. Hwu. 2010. "Biocompatibility of Fe_3O_4 Nanoparticles Evaluated by in Vitro Cytotoxicity Assays Using Normal, Glia and Breast Cancer Cells." *Nanotechnology* 21(7): 075102–0759. doi:10.1088/0957-4484/21/7/075102.

Armstrong, C. M., R. P. Swenson, and S. R. Jr Taylor. 1982. "Block of Squid Axon K Channels by Internally and Externally Applied Barium Ions." *The Journal of General Physiology* 80(5): 663–682. doi:10.1085/jgp.80.5.663.

Beedle, A. M., J. Hamid, and G. W. Zamponi. 2002. "Inhibition of Transiently Expressed Low- and High-Voltage-Activated Calcium Channels by Trivalent Metal Cations." *The Journal of Membrane Biology* 187: 225–238. doi:10.1007/s00232-001-0166-2.

Bérubé, J., D. Caouette, and P. Daleau. 2001. "Hydrogen Peroxide Modifies the Kinetics of hERG Channel Expressed in a Mammalian Cell Line." *Journal of Pharmacology and Experimental Therapeutics* 297: 96–102. http://jpet.aspetjournals.org/content/297/1/96.long.

Bulte, J. W. M., T. Douglas, B. Witwer, S. C. Zhang, E. Strable, B. K. Lewis, H. Zywicke, B. Miller, P. van Gelderen, and B. M. Moskowitz. 2001. "Magnetodendrimers Allow Endosomal Magnetic Labeling and in Vivo Tracking of Stem Cells." *Nature Biotechnology* 19(12): 1141–1147. doi:10.1038/nbt1201-1141.

Chen, M. X., R. M. Helliwell, and J. J. Clare. 2009. "In Vitro Profiling against Ion Channels beyond hERG as an Early Indicator of Cardiac Risk." *Current Opinion in Molecular Therapeutics* 11: 269–281. https://www.ncbi.nlm.nih.gov/pubmed/19479660.

Colombo, M., S. Carregal-Romero, M. F. Casula, L. Gutiérrez, M. P. Morales, I. B. Böhm, J. T. Heverhagen, D. Prosperi, and W. J. Parak. 2012. "Biological Applications of Magnetic

Nanoparticles." *Chemical Society Reviews* 41(11): 4306–4334. doi:10.1039/c2cs15337h.

Dissanayake, N. M., K. M. Current, and S. O. Obare. 2015. "Mutagenic Effects of Iron Oxide Nanoparticles on Biological Cells." *International Journal of Molecular Sciences* 16(10): 23482–23516. doi:10.3390/ijms161023482.

Duguet, E., S. Vasseur, S. Mornet, and J. M. Devoisselle. 2006. "Magnetic Nanoparticles and Their Applications in Medicine." *Nanomedicine* 1(2): 157–168. doi:10.2217/17435889.1.2.157.

Elinder, F., and P. Arhem. 2003. "Metal Ion Effects on Ion Channel Gating." *Quarterly Reviews of Biophysics* 36(4): 373–427. doi:10.1017/S0033583504003932.

Fermini, B., and A. A. Fossa. 2003. "The Impact of Drug-Induced QT Interval Prolongation on Drug Discovery and Development." *Nature Reviews Drug Discovery* 2(6): 439–447. doi:10.1038/nrd1108.

Fernandez, D., A. Ghanta, K. I. Kinard, and M. C. Sanguinetti. 2005. "Molecular Mapping of a Site for Cd^{2+}-Induced Modification of Human Ether-à-Go-Go-Related Gene (hERG) Channel Activation." *The Journal of Physiology* 567(3): 737–755. doi:10.1113/jphysiol.2005.089094.

Ficker, E., W. Jarolimek, and A. M. Brown. 2001. "Molecular Determinants of Inactivation and Dofetilide Block in Ether a-Go-Go (EAG) Channels and EAG-Related K(+) Channels." *Molecular Pharmacology* 60(6): 1343–1348. doi:10.1124/mol.60.6.1343.

Food and Drug Administration, HHS. 2005. "International Conference on Harmonisation (ICH) Guidance on S7B Nonclinical Evaluation of the Potential for Delayed Ventricular Repolarization (QT Interval Prolongation). Human Pharmaceuticals Availability. Notice. *Federal Register* 70: 61133–61134. http://www.ich.org/fileadmin/Public_Web_Site/ICH_Products/Guidelines/Safety/S7B/Step4/S7B_Guideline.pdf.

Gu, Z., L. D. Plant, X. Y. Meng, J. M. Perez-Aguilar, Z. Wang, M. Dong, D. E. Logothetis, and R. Zhou. 2018. "Exploring the Nanotoxicology of MoS_2: A Study on the Interaction of MoS_2 Nanoflakes and K^+ Channels." *ACS Nano* 12(1): 705–717. doi:10.1021/acsnano.7b07871.

Gualdani, R., M. M. Cavalluzzi, F. Tadini-Buoninsegni, M. Convertino, P. Gailly, A. Stary-Weinzinger, and G. Lentini. 2018. "Molecular Insights into hERG Potassium Channel Blockade by Lubeluzole." *Cellular Physiology and Biochemistry* 45(6): 2233–2245. doi:10.1159/000488169.

Gualdani, R., F. Tadini-Buoninsegni, M. Roselli, I. Defrenza, M. Contino, N. A. Colabufo, and G. Lentini. 2015. "Inhibition of hERG Potassium Channel by the Antiarrhythmic Agent Mexiletine and its Metabolite m-Hydroxymexiletine." *Pharmacology Research & Perspectives* 3: E 00160. doi:10.1002/prp2.160.

Gupta, A. K., and M. Gupta. 2005. "Synthesis and Surface Engineering of Iron Oxide Nanoparticles for Biomedical Applications." *Biomaterials* 26(18): 3995–4021. doi:10.1016/j.biomaterials.2004.10.012.

Hafeli, U. O., J. S. Riffle, L. Harris-Shekhawat, A. Carmichael-Baranauskas, F. Mark, J. P. Dailey, and D. Bardenstein. 2009. "Cell Uptake and in Vitro Toxicity of Magnetic Nanoparticles Suitable for Drug Delivery." *Molecular Pharmaceutics* 6: 1417–1428. doi:10.1021/mp900083m.

Horwitz, L. D., and E. A. Rosenthal. 1999. "Iron-Mediated Cardiovascular Injury." *Vascular Medicine* 4(2): 93–99. doi:10.1191/135886399676588477.

Huber, D.L. 2005. "Synthesis, Properties, and Applications of Iron Nanoparticles." *Small* 1(5): 482–501. doi:10.1002/smll.200500006.

Hussain, S. M., K. L. Hess, J. M. Gearhart, K. T. Geiss, and J. J. Schlager. 2005. "In Vitro Toxicity of Nanoparticles in BRL 3A Rat Liver Cells." *Toxicology in Vitro: An International Journal Published in Association with Bibra* 19(7): 975–983. doi:10.1016/j.tiv.2005.06.034.

Iancu, T. C., H. Shiloh, G. Link, E. R. Bauminger, A. Pinson, and C. Hershko. 1987. "Ultrastructural Pathology of Iron-Loaded Rat Myocardial Cells in Culture." *British Journal of Experimental Pathology* 68: 53–65. https://www.ncbi.nlm.nih.gov/pmc/articles/PMC2012992/.

Jeng, H. A., and J. Swanson. 2006. "Toxicity of Metal Oxide Nanoparticles in Mammalian Cells." *Journal of Environmental Science and Health. Part A, Toxic/Hazardous Substances & Environmental Engineering* 41: 2699–2711. doi:10.1080/10934520600966177.

Johannsen, M., U. Gneveckow, K. Taymoorian, B. Thiesen, N. Waldöfner, R. Scholz, K. Jung, A. Jordan, P. Wust, and S. A. Loening. 2007. "Morbidity and Quality of Life During Thermotherapy Using Magnetic Nanoparticles in Locally Recurrent Prostate Cancer: Results of a Prospective Phase I Trial." *International Journal of Hyperthermia* 23(3): 315–323. doi:10.1080/02656730601175479.

Johnson, J. P., J. R. Balser, and P. B. Bennett. 2001. "A Novel Extracellular Calcium Sensing Mechanism in Voltage-Gated Potassium Ion Channels." *The Journal of Neuroscience* 21(12): 4143–4153. doi:10.1523/JNEUROSCI.21-12-04143.2001.

Johnson, J. P., F. M. Mullins, and P. B. Bennett. 1999. "Human Ether-à-Go-Go-Related Gene K^+ Channel Gating Probed with Extracellular Ca^{2+}: Evidence for Two Distinct Voltage Sensors." *The Journal of General Physiology* 113(4): 565–580. doi:10.1085/jgp.113.4.565.

Kremastinos, D. T., and D. Farmakis. 2011. "Iron Overload Cardiomyopathy in Clinical Practice." *Circulation* 124(20): 2253–2263. doi:10.1161/CIRCULATIONAHA.111.050773.

Kudaibergenova, M., L. L. Perissinotti, and S. Y. Noskov. 2018. "Lipid Roles in hERG Function and Interactions with Drugs." *Neuroscience Letters* 700:70–77. doi:10.1016/j.neulet.2018.05.019.

Kuryshev, Y. A., G. M. Brittenham, H. Fujioka, P. Kannan, C. C. Shieh, S. A. Cohen, and A. M. Brown. 1999. "Decreased Sodium and Increased Transient Outward Potassium Currents in Iron-Loaded Cardiac Myocytes." *Circulation* 100: 675–683. doi:10.1161/01.CIR.100.6.675.

Leifert, A., Y. Pan, A. Kinkeldey, F. Schiefer, J. Setzler, O. Scheel, H. Lichtenbeld, et al. 2013. "Differential hERG Ion Channel Activity of Ultrasmall Gold Nanoparticles." *Proceedings of the National Academy of Sciences of Sciences* 110(20): 8004–8009. doi:10.1073/pnas.1220143110. .

Lin, M. C., and D. M. Papazian. 2007. "Differences between Ion Binding to Eag and HERG Voltage Sensors Contribute to Differential Regulation of Activation and Deactivation Gating." *Channels (Austin)* 1(6): 429–437. doi:10.4161/chan.1.6.5760.

Maier-Hauff, K., F. Ulrich, D. Nestler, H. Niehoff, P. Wust, B. Thiesen, H. Orawa, V. Budach, and A. Jordan. 2011. "Jordan, Efficacy and Safety of Intratumoral Thermotherapy Using Magnetic Iron-Oxide Nanoparticles Combined with External Beam Radiotherapy on Patients with Recurrent Glioblastoma Multiforme." *Journal of Neuro-Oncology* 103(2): 317–324. doi:10.1007/s11060-010-0389-0.

McLaughlin, S. 1989. "The Electrostatic Properties of Membranes." *Annual Review of Biophysics and Biophysical Chemistry* 18: 113–136. doi:10.1146/annurev.bb.18.060189.000553.

Mitcheson, J. S., J. Chen, M. Lin, C. Culberson, and M. C. Sanguinetti. 2000. "A Structural Basis for Drug-Induced Long QT Syndrome." *Proceedings of the National Academy of Sciences of Sciences* 97(22): 12329–12333. doi:10.1073/pnas.210244497.

Moore, T. L., L. Rodriguez-Lorenzo, V. Hirsch, S. Balog, D. Urban, C. Jud, B. Rothen-Rutishauser, M. Lattuada, and A. Petri-Fink. 2015. "Nanoparticle Colloidal Stability in Cell Culture Media and Impact on Cellular Interactions." *Chemical Society Reviews* 44(17): 6287–6305. doi:10.1039/C4CS00487F.

Oshiro, S., M. S. Morioka, and M. Kikuchi. 2011. "Dysregulation of Iron Metabolism in Alzheimer's Disease, Parkinson's Disease, and Amyotrophic Lateral Sclerosis." *Advances in Pharmacological Sciences* 2011: 1. doi:10.1155/2011/378278.

Parkes, J. G., Y. Liu, J. B. Sirna, and D. M. Templeton. 2000. "Changes in Gene Expression with Iron Loading and Chelation in Cardiac Myocytes and Non-Myocytic Fibroblasts." *Journal of Molecular and Cellular Cardiology* 32(2): 233–246. doi:10.1006/jmcc.1999.1068.

Piscopo, S., and E. R. Brown. 2018. "Zinc Oxide Nanoparticles and Voltage-Gated Human K_V11.1 Potassium Channels Interact Though a Novel Mechanism." *Small* 14(15): 1703403. doi:10.1002/smll.201703403.

Po, S. S., D. W. Wang, I. C. Yang, J. P. Jr Johnson, L. Nie, and P. B. Bennett. 1999. "Modulation of hERG Potassium Channels by Extracellular Magnesium and Quinidine." *Journal of Cardiovascular Pharmacology* 33(2): 181–185. doi:10.1097/00005344-199902000-00002.

Sanguinetti, M. C., M. E. Curran, A. Zou, J. Shen, P. S. Spector, D. L. Atkinson, and M. T. Keating. 1996. "Coassembly of K(V)LQT1 and minK (IsK) Proteins to Form Cardiac I(Ks) Potassium Channel." *Nature* 384(6604): 80–83. doi:10.1038/384080a0.

Sanguinetti, M. C., C. Jiang, M. E. Curran, and M. T. Keating. 1995. "A Mechanistic Link between an Inherited and an Acquired Cardiac Arrhythmia: hERG Encodes the I_{Kr} Potassium Channel." *Cell* 81(2): 299–307. doi:10.1016/0092-8674(95)90340-2.

Singh, N., G. J. S. Jenkins, R. Asadi, and S. H. Doaka. 2010. "Potential Toxicity of Superparamagnetic Iron Oxide Nanoparticles (SPION)." *Nano Reviews* 1: 5358. doi:10.3402/nano.v1i0.5358.

Stankiewicz, J. M., and S. D. Brass. 2009. "Role of Iron in Neurotoxicity: A Cause for Concern in the Elderly?" *Current Opinion in Clinical Nutrition and Metabolic Care* 12: 22–29. doi:10.1097/MCO.0b013e32831ba07c.

Stroh, A., C. Zimmer, C. Gutzeit, M. Jakstadt, F. Marschinke, T. Jung, H. Pilgrimm, and T. Grune. 2004. "Iron Oxide Particles for Molecular Magnetic Resonance Imaging Cause Transient Oxidative Stress in Rat Macrophages." *Free Radical Biology and Medicine* 36(8): 976–984. doi:10.1016/j.freeradbiomed.2004.01.016.

Taglialatela, M., P. Castaldo, S. Iossa, A. Pannaccione, A. Fresi, E. Ficker, and L. Annunziato. 1997. "Regulation of the Human Ether-a-Gogo Related Gene (HERG) K^+ Channels by Reactive Oxygen Species." *Proceedings of the National Academy of Sciences of Sciences* 94(21): 11698–11703. doi:10.1073/pnas.94.21.11698.

Tsushima, R. G., A. D. Wickenden, R. A. Bouchard, G. Y. Oudit, P. P. Liu, and P. H. Backx. 1999. "Modulation of Iron Uptake in Heart by L-Type Ca^{2+} Channel Modifiers: Possible Implications in Iron Overload." *Circulation Research* 84(11): 1302–1309. doi:10.1161/01.RES.84.11.1302.

Veranth, J. M., E. G. Kaser, M. M. Veranth, M. Koch, and G. S. Yost. 2007. "Cytokine Responses of Human Lung Cells (BEAS-2B) Treated with Micron-Sized and Nanoparticles of Metal Oxides Compared to Soil Dusts." *Particle and Fibre Toxicology* 4(1): 2. doi:10.1186/1743-8977-4-2.

Winegar, R. D., R. Kelly, and J. B. Lansman. 1991. "Block of Current through Single Calcium Channels by Fe, Co, and Ni. Location of the Transition Metal Binding Site in the Pore." *The Journal of General Physiology* 97(2): 351–367. doi:10.1085/jgp.97.2.351.

Zhang, A. S., and C. A. Enns. 2009. "Molecular Mechanisms of Normal Iron Homeostasis." *Hematology* 2009: 207–214. doi:10.1182/asheducation-2009.1.207.

Zhou, Z., Q. Gong, B. Ye, Z. Fan, J.C. Makielski, G. A. Robertson, and C. T. January. 1998. "Properties of HERG Channels Stably Expressed in HEK 293 Cells Studied at Physiological Temperature." *Biophysical Journal* 74(1): 230–241. doi:10.1016/S0006-3495(98)77782-3.